Correction

PHYSIOLOGY

Correction for "Integrated 3D view of postmating responses by the *Drosophila melanogaster* female reproductive tract, obtained by micro-computed tomography scanning," by Alexandra L. Mattei, Mark L. Riccio, Frank W. Avila, and Mariana F. Wolfner, which appeared in issue 27, July 7, 2015, of *Proc Natl Acad Sci USA* (112:8475–8480; first published June 3, 2015; 10.1073/pnas.1505797112).

The authors note that Fig. 1 and its corresponding legend appeared incorrectly. The corrected figure and its corrected legend appear below. This error does not affect the conclusions of the article.

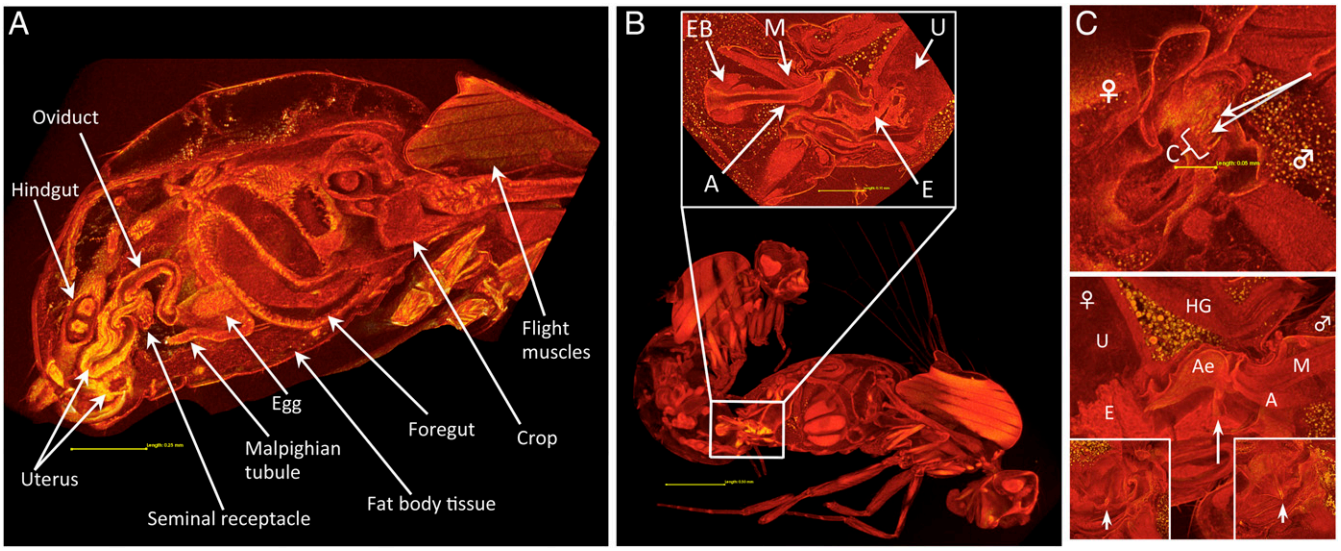

Fig. 1. Micro-CT scans of copulating *Drosophila* visualized in three dimensions. (*A*) Abdomen of a virgin female, showing details of RT anatomy. A mid-longitudinal slice of a Canton S female is shown; ovaries, spermathecae, and parovaria are lateral to this slice and not visible in this section (Fig. S1). (*B*) Copulating pair at 10 min ASM. (*Inset*) Close-up view of the reproductive anatomy at a voxel size of 597 nm. Flies are virtually sliced midlongitudinally to reveal their internal organs. (*C*) Copulating flies scanned at 10 min ASM show male claspers ("c") interdigitate with the female vaginal teeth (bracket and arrows) at the top of the RT opening (*Upper*) and apparent copulatory damage to the female intima (arrows) caused by the male's aedeagus (*Lower*). Arrow in *Lower* panel of *C* points to the puncture of the female by the dorsal branch of the aedeagus. The insets in this panel show the same place in two slightly different focal planes centered on the tip of the dorsal branch of the aedeagus. A, aedeagal apodeme; Ae, aedeagus; E, ejaculate, EB, ejaculatory bulb; M, muscle fiber; U, uterus, HG, hindgut. Delineation of the aedeagal apodeme is shown in Fig. S2; in that figure, "E" designates aedeagus. Yellow indicates the highest density, and red indicates the lowest density. Scale bars: *A*, 0.25 mm; *B*, 0.5 mm; *C* and *B* (*Inset*), 0.1 mm.

www.pnas.org/cgi/doi/10.1073/pnas.1708561114

CORRECTION

Integrated 3D view of postmating responses by the *Drosophila melanogaster* female reproductive tract, obtained by micro-computed tomography scanning

Alexandra L. Mattei[a,1], Mark L. Riccio[b,2], Frank W. Avila[a,2], and Mariana F. Wolfner[a,3]

[a]Department of Molecular Biology and Genetics, Cornell University, Ithaca, NY 14853; and [b]Institute of Biotechnology, Cornell University, Ithaca, NY 14853

Edited by David L. Denlinger, Ohio State University, Columbus, OH, and approved May 7, 2015 (received for review March 24, 2015)

Physiological changes in females during and after mating are triggered by seminal fluid components in conjunction with female-derived molecules. In insects, these changes include increased egg production, storage of sperm, and changes in muscle contraction within the reproductive tract (RT). Such postmating changes have been studied in dissected RT tissues, but understanding their coordination in vivo requires a holistic view of the tissues and their interrelationships. Here, we used high-resolution, multiscale micro-computed tomography (CT) scans to visualize and measure postmating changes in situ in the *Drosophila* female RT before, during, and after mating. These studies reveal previously unidentified dynamic changes in the conformation of the female RT that occur after mating. Our results also reveal how the reproductive organs temporally shift in concert within the confines of the abdomen. For example, we observed chiral loops in the uterus and in the upper common oviduct that relax and constrict throughout sperm storage and egg movement. We found that specific seminal fluid proteins or female secretions mediate some of the postmating changes in morphology. The morphological movements, in turn, can cause further changes due to the connections among organs. In addition, we observed apparent copulatory damage to the female intima, suggesting a mechanism for entry of seminal proteins, or other exogenous components, into the female's circulatory system. The 3D reconstructions provided by high-resolution micro-CT scans reveal how male and female molecules and anatomy interface to carry out and coordinate mating-dependent changes in the female's reproductive physiology.

reproduction | micro-CT scans | uterus | seminal proteins | oviduct

Mating induces physiological changes in females that enhance fertility. Many of these changes result from the transfer of seminal fluid, a complex chemical mixture containing sperm, male-derived molecules, and membranous vesicles (1–6), acting in the context of, and in conjunction with, female molecules and physiology. In insects and mammals, examples include seminal components that induce contraction of the female reproductive tract (RT) musculature (7–10), stimulate ovulation (11–13), regulate semen coagulation (14, 15), aid sperm movement and storage in the female RT (16, 17), and modulate female immune responses postmating (18, 19).

Drosophila melanogaster is a powerful system with which to dissect how male-derived molecules interact with female physiology to cause the cascade of postmating responses required for fertility. *Drosophila* males transfer >200 different seminal fluid proteins (SFPs) to females during mating (19–21). Within the female RT, SFPs induce a series of conformational changes of the uterus (16, 22). Specific SFPs increase ovulation and oviposition rates (12, 13, 23), promote sperm storage (16, 24, 25), increase feeding (26), decrease intestinal transit rates (27, 28), and increase synaptic development at female RT neuromuscular junctions (10). Although much is known about the molecules and interactions that mediate these female postmating responses, next to nothing is known about the physical mechanics of the postmating changes and their response to male and female molecules.

The physical act of mating, SFPs, and sperm receipt each modulate the release of signaling molecules in the *Drosophila* female RT (29). The *Drosophila* female RT is a complex system whose subregions differ in function and in the release and reuptake of signaling molecules; each region has a characteristic temporal and spatial identity postmating. Thus, postmating physiological changes are not simply a sequence of independent events but rather a coordinated process required for optimal fertility. Previous studies carried out on dissected tissues or specimens did not allow observation of the interactions and coordination among RT organs in situ within mating, or mated, flies.

To visualize spatially the coordinated and concurrent organ rearrangements within the confines of the female abdomen during insemination through to egg laying, we used high-resolution, multiscale micro-computed tomography (CT) scans. These scans give a holistic 3D view of the interrelationship among reproductive organs in situ, as females respond to mating and its chemical components. With views ranging from 400-nm to 4-μm voxel sizes of the interior of female flies before, during, and at several times after mating, we observed looping, opening/closing, and repositioning of RT organs within the female. These data allow us to revisit, and newly define, effects of male and female molecules on female postmating physiology.

Significance

Our high-resolution, multiscale micro-computed tomography scans of *Drosophila* provide the first 3D view, to our knowledge, of the in situ morphological changes that occur in a female insect's reproductive tract (RT) during and after mating. By means of this holistic analysis, we determined how the postmating reproductive events of ovulation, egg movement, sperm storage, sperm release, and fertilization are coordinated. We observed and quantified phenomena not detected in prior studies of dissected materials. These phenomena included coordinated looping and unlooping of the uterus and oviducts, and a potential mating-induced trauma in the female RT. This new perspective allowed us to revisit experimentally, and newly define, the effects of male- and female-secreted molecules on female postmating physiology.

Author contributions: A.L.M., F.W.A., and M.F.W. designed research; A.L.M., M.L.R., and F.W.A. performed research; A.L.M., M.L.R., F.W.A., and M.F.W. analyzed data; and A.L.M., M.L.R., F.W.A., and M.F.W. wrote the paper.

The authors declare no conflict of interest.

This article is a PNAS Direct Submission.

See Commentary on page 8168.

[1]Present address: Department of Molecular and Cellular Biology, Harvard University, Cambridge, MA 02138.

[2]M.L.R. and F.W.A. contributed equally to this work.

[3]To whom correspondence should be addressed. Email: mfw5@cornell.edu.

This article contains supporting information online at www.pnas.org/lookup/suppl/doi:10.1073/pnas.1505797112/-/DCSupplemental.

Results and Discussion

A brief outline of the progression of events initiated by mating is necessary before we present, in the following sections, how the female's RT changes with time after copulation.

During a typical *D. melanogaster* mating, SFPs are transferred to females beginning at 3 min after the start of mating (ASM) (30, 31). SFPs from the male ejaculatory bulb coagulate into a hardened mass [the posterior mating plug (MP)] at 5 min ASM, whereas SFPs primarily from the male accessory gland condense into an anterior MP at 20 min ASM (30, 32). Sperm are transferred between these events at 8 min ASM (33, 34), and their storage in the female begins at ~25 min ASM (34). We examined female RT tissues in situ during copulation (10 min ASM) at time points immediately after mating [35–90 min ASM (during sperm storage and the start of ovulation, respectively)], as well as later, when females are actively laying eggs and sperm storage is complete (3–8 h ASM). We then examined effects of specific male or female components on the tissues' behaviors.

Mating Flies Couple Precisely, with the Female's Vaginal Teeth Interdigitating with the Male's Claspers. We flash-froze virgin females, mating pairs *in copula* at 10 min ASM (Fig. 1 and Movie S1), and mated females at 35 min, 90 min, 3 h, 5 h, and 8 h ASM, and then examined them by ultra-high-resolution CT scans (400-nm and 597-nm voxel sizes). An overview CT scan of the internal virgin female reproductive anatomy is shown in Fig. 1*A*. A region of high density in the lumen of the posterior uterus is seen only in mated females ("E" in Fig. 1*B*, *Inset*). Scans of females mated to males depleted for particular ejaculate components (Table S1 and below) suggest that this high-density region corresponds to ejaculatory bulb secretions that form the posterior MP. At the site of male/female genital contact in the pair of flies *in copula*, our scans revealed directly, and for the first time to our knowledge, that the female's vaginal teeth interlock with the male's claspers. This interdigitation could keep the animals tightly and correctly coupled during mating. There is also the possibility that it could act as a stimulatory signal on the female [Fig. 1 *B* (*Inset*) and *C*].

Male's Intromittent Organ Pierces the Female Fly's Vagina. Our scans of fly pairs *in copula* revealed that the tip of the aedeagus, the male's intromittent organ, appeared to extend through the dorsal posterior vaginal wall (Fig. 1*C*), causing copulatory damage in the region. Such wounding could occur when the muscle that attaches to the curved posterior end of the aedeagus contracts [Fig. 1 *B* (*Inset*) and *C*]. We see a single penetration of the female intima, consistent with a phallotreme structure for *D. melanogaster* analogous to the structure seen for *Drosophila eugracilis*, another species that shows copulatory wounding (35). The purpose or effect of such copulatory wounding is not clear. One possibility is that it provides a means for male seminal components to enter the female's circulatory system. Some SFPs enter the circulatory system in the first few minutes of mating (31, 36). *D. melanogaster* males also transfer membrane-bound vesicles (5), and likely transfer RNAs as was reported for *Drosophila mojavensis* males (37); such male constituents could also potentially gain access to the female's circulation through the copulatory wound. Damage or entry of exogenous substances into the female might also contribute to the induction of antimicrobial gene expression that occurs after mating (38–40), or might serve as an entry route for pathogens (41).

We next examined how the female's RT changes with time after copulation. We discuss this by following the path of oocyte transit from ovary, through lateral and common oviducts, to uterus.

Mating Triggers a Clutch-Like Wave of Egg Production. We examined ovarian morphology before, during, and after mating (Fig. 2 and Fig. S3). Ovaries of virgin and mated females at 10, 15, 35, and 90 min ASM are full of both immature and mature oocytes (Fig. 2*A*, *b*–*e*). Ovaries of females at 3 and 5 h ASM, when egg production is high, have expanded to fill the majority of the abdomen (Fig. 2*A*, *f* and *g*). Of the six females scanned at 8 h ASM, the ovaries of two contained mature oocytes and many immature oocytes (Fig. 2*A*, *h* and *i*). Three had ovaries devoid of mature oocytes (Fig. 2*A*, *j*–*l*), and one had a mature oocyte in only one ovary. Ovaries lacking mature oocytes were noticeably smaller than the ovaries of virgins.

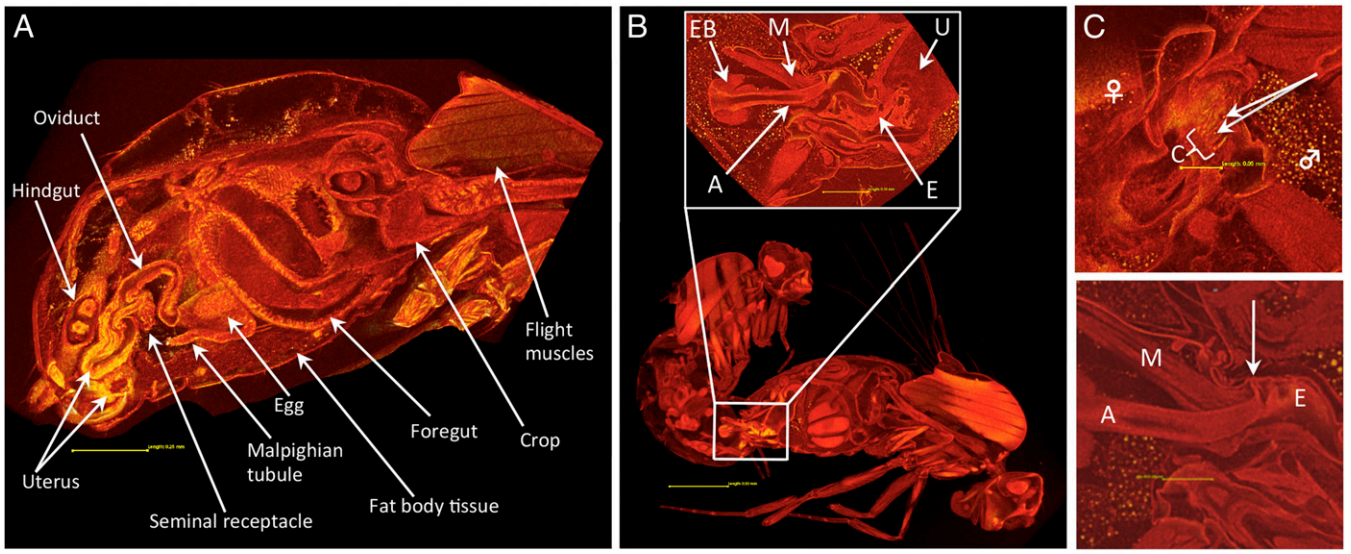

Fig. 1. Micro-CT scans of copulating *Drosophila* visualized in three dimensions. (*A*) Abdomen of a virgin female, showing details of RT anatomy. A midlongitudinal slice of a Canton S female is shown; ovaries, spermathecae, and parovaria are lateral to this slice and not visible in this section (Fig. S1). (*B*) Copulating pair at 10 min ASM. (*Inset*) Close-up view of the reproductive anatomy at a voxel size of 597 nm. Flies are virtually sliced midlongitudinally to reveal their internal organs. (*C*) Copulating flies scanned at 10 min ASM show male claspers ("c") interdigitate with the female vaginal teeth (bracket and arrows) at the top of the RT opening (*Upper*) and apparent copulatory damage to the female intima (arrow) caused by the male's aedeagus (*Lower*). Delineation of the aedeagus is shown in Fig. S2. Yellow indicates the highest density, and red indicates the lowest density. A, aedeagus; E, ejaculate; EB, ejaculatory bulb; M, muscle fiber; U, uterus. (Scale bars: *A*, 0.25 mm; *B*, 0.5 mm; *C* and *B* (*Inset*), 0.1 mm.)

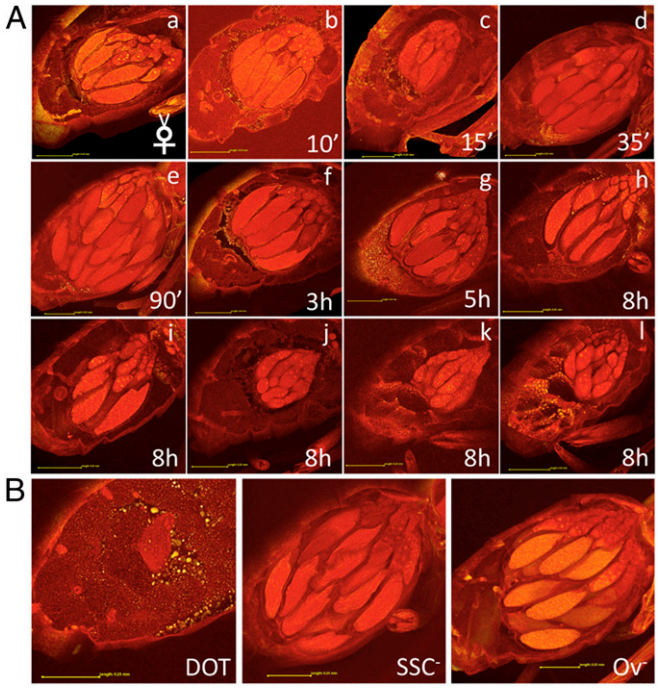

Fig. 2. Progression of morphological changes of ovaries during and after mating. (*A*) Ovaries of a virgin female (♀) are full of immature and maturing eggs, and maintain a similar size during mating (10 and 15 min ASM). More eggs begin to mature soon after mating (35 min ASM); they fill the ovaries, which increase in size (90 min and 3 h ASM). Females begin actively laying eggs by 5–8 h ASM. By 8 h ASM, some ovaries still contain mature eggs (*h* and *i*), whereas others are completely devoid of mature eggs (*j*–*l*). (*B*) Ovaries of eggless (DOT) females are severely reduced in size and lack oocytes at 90 min ASM; the space these ovaries normally occupy is filled with fat body. At 90 min ASM, the ovaries of SSC$^-$ females or of normal females mated to Ov$^-$ males show accumulation of excess (unovulated) mature oocytes. (Scale bar: 0.25 mm.)

Considered together, the progression of *D. melanogaster* ovarian morphologies from virgin females through mated females at 8 h ASM, as well as the overall paucity of mature oocytes in the ovaries of females at 8 h ASM, suggests some clutch-like characteristics to (at least) the initial postmating bout of egg production/laying. Our data also show that a certain number of oocytes mature in the ovaries of virgin females before the onset of postmating egg laying and are ovulated before the next set of oocytes matures; this pattern is consistent with predictions for how SFPs stimulate oogenesis (42, 43). Synchronized or clutch-like egg production has not previously been reported for *D. melanogaster*. Intriguingly however, synchronized egg production occurs in some other insects. For example, females of some *Drosophila repleta* species mature their eggs in batches, and female *Drosophila pseudoobscura* also do so to some extent (44), and synchronized egg production triggered by mating results in female mosquitoes laying a clutch of eggs (45). It will be fascinating to compare effects of mating on the dynamics and synchronicity of oogenesis and egg maturation across insect species, including the genus *Drosophila.* It will also be interesting to examine whether *D. melanogaster* egg production continues to display cyclicity and batch-like characteristics after the initial postmating cycle, perhaps to allow coordination with circadian cues or feeding cycles.

Male and Female Secretions Prevent Overfilling of Ovaries with Eggs. Seminal proteins like ovulin, and female spermathecal secretory cell (SSC) secretions regulate postmating ovulation levels in *Drosophila* (10, 12, 46–48). Given the stimulation of oogenesis by mating, one might expect that in the absence of male or female molecules that stimulate ovulation, the ovaries might overfill with mature oocytes. Our micro-CT scan datasets provide evidence for such an effect. In females whose SSCs were disabled (SSC$^-$) or in normal females mated to ovulin-deficient males (Ov$^-$), the ovaries were abnormally full of mature oocytes (Fig. 2*B*, SSC$^-$ and Ov$^-$), stacked on top of each other. This was never observed in WT matings.

Overfilling of Ovaries with Eggs Does Not Alter the Conformation of the Uterus and Oviducts. As will be described below, the oviducts and uterus, through which oocytes pass, undergo conformational changes after mating. Interestingly, despite the engorgement of the ovaries in the absence of ovulin or SSC secretions, the remainder of these females' RTs showed normal conformations (Figs. 3 and 4). This suggested that the germ cell contents of the ovary do not exert major effects on the other RT tissues. To test this hypothesis, we examined ovarian, uterine, and oviduct conformation in mated females without oocytes [daughters of *tudor* (DOT) (49)] (Figs. 2–4 and Table S1). These females showed normal uterine (Fig. 4, DOT) and oviductal (Fig. 3*B*, DOT) morphology at 90 min ASM, even though their ovaries, lacking oocytes, were much smaller than normal (Fig. 2*B*, DOT). Thus, the presence or absence of mature oocytes does not impact oviductal and uterine conformations or position postmating.

Mating and Seminal Proteins Cause Coordinated Looping and Straightening of the Oviducts. In the upper common oviduct of virgin females, we observed a chiral counterclockwise loop (Fig. 3*A*, *a*). This conformation is maintained in mated females at 10, 15, and 35 min ASM (Fig. 3*A*, *b*–*d*). However, by 90 min ASM, the time at which postmating ovulation initiates (10, 12), the loop has uncoiled (Fig. 3*A*, *e*). The oviduct remains straight at 3 h ASM (Fig. 3*A*, *f*), but by 5 h ASM (Fig. 3*A*, *g*), and continuing at 8 h ASM (Fig. 3*A*, *j* and *k*), the oviduct appeared to have recoiled partially to an intermediate conformation (Fig. 3*A*). At 8 h ASM, we observed female-to-female variation: Of the four females with an egg in the uterus at 8 h ASM, the oviduct was in a chiral loop in two (e.g., Fig. 3*A*, *l*), in an intermediate conformation in one (Fig. 3*A*, *k*), and straight in one (Fig. 3*A*, *i*). In the two females without an egg in their uterus at 8 h ASM, the oviduct was in the intermediate conformation in one and straight in the other (Fig. 3*A*, *j* and *h*, respectively).

Ovulation is stimulated by the SFP ovulin, which relaxes oviduct muscles via increased octopaminergic signaling (10, 12, 13, 48). To test whether ovulin's action causes the straightening of the oviduct observed at 90 min ASM, we examined oviducts of females mated to ovulin-deficient males. Oviducts in females that did not receive ovulin retained their loops at 90 min ASM, in contrast to controls (Fig. 3*B*, Ov$^-$). The failure of the oviduct to straighten in the absence of ovulin was not due to the accumulation of unovulated oocytes, because the oviducts of SSC$^-$ females, which also accumulate unovulated oocytes, straighten normally (Fig. 3*B*, SSC$^-$). Thus, our data show that uncoiling of the oviductal loop is a result of ovulin's effect on muscle contraction.

Mating Causes Changes in Uterine Volume, Shape, and Positioning. Uteri of unmated females were reported previously, based on dissected materials, to be "closed" and "S-shaped" (22). Our 3D examination showed that the closed uterus actually loops in the horizontal *x*–*y* plane, rather than being a flat S-shape in the vertical *y*–*z* plane (Figs. 1*A* and 4 and Fig. S4*A*). Earlier studies on dissected materials also reported that after mating, the uterus undergoes a series of morphological changes that "open" its lumen (22). We observed this progression in micro-CT scans taken at 10, 15, 35 and 90 min ASM (internal structures are labeled in Fig. 1*A*). Consistent with prior observations (22), uterine expansion did not require receipt of sperm by the female [Fig. 4; females mated to spermless, sons of *tudor* (SOT) males].

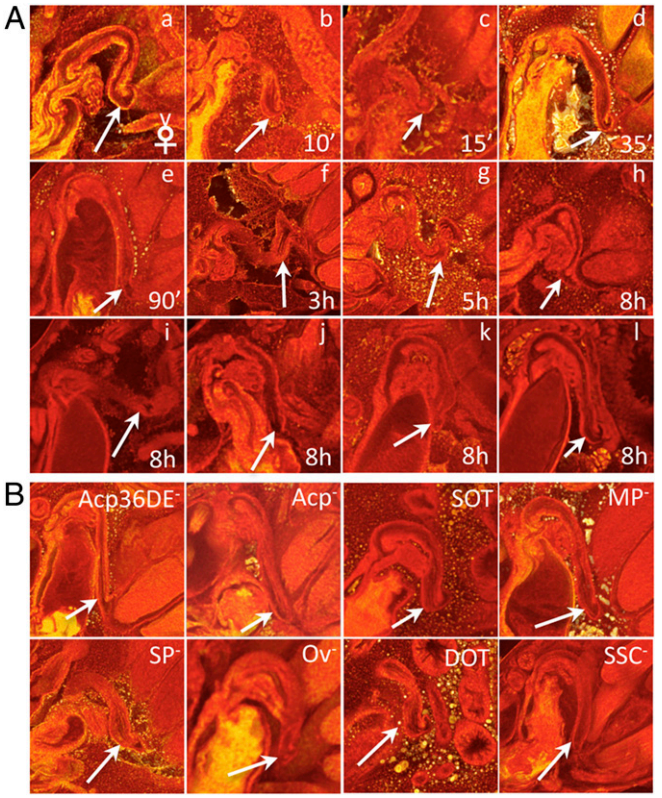

Fig. 3. Morphology of the upper common oviduct (arrows) at the indicated times ASM. (*A*) Upper common oviducts show a chiral loop (arrows) at 0, 10, 15, and 35 min ASM (*a*–*d*). (*e*) At 90 min ASM, the oviducts start to relax and show no loop. Likewise, the oviduct is relaxed at 3 h ASM (*f*) and at 8 h ASM when an egg is positioned in the lateral oviduct (*h*) or when it has descended into the uterus (*i*). (*l*) Loop reforms during egg laying, as seen at 8 h ASM when an egg is in the uterus. A state intermediate between looped and relaxed is seen at 5 (*g*) and 8 (*j* and *k*) h ASM. (*B*) Upper common oviduct (arrows) is straight at 35 min ASM in mates of Acp36DE^{-} males and males lacking all Acps (Acp^{-}), but has a loop in females mated to males that produce Acps but not sperm (SOT). Mates of *pEBme* knockdown males (MP^{-}) show partial relaxation in the oviduct at 35 min ASM. At 90 min ASM, mates of males lacking sex peptide (SP^{-}) show normal oviduct relaxation, mates of Ov^{-} males show no relaxation in the oviduct, an eggless female (DOT) shows no relaxation in the oviduct, and SSC^{-} females have relaxed oviducts. (Scale bar: 0.25 mm.)

The 3D information gained from our scans allowed us to calculate the magnitude of the change in uterine volume during its expansion (*SI Materials and Methods*, Fig. S5, and Table S2). Interestingly, the uterus reaches its largest size at 90 min ASM, before egg entry into the uterus; uterine volume at this time is greater than the uterine volume of a uterus holding an egg. We suggest that the uterus balloons to accept the egg and subsequently contracts to hold the egg in place for fertilization. An egg within the uterus is thus held snugly, with its dorsal appendages sticking into the oviduct. The egg's micropyle is positioned near the entrances to the sperm storage organs, presumably facilitating fertilization. Uterine ballooning before egg entry also facilitates opening the entryways to the sperm storage organs to store sperm efficiently (22). It is also possible that this ballooning prepares the RT for later events, by stretching the epithelia and muscles to accommodate more easily eggs that will descend when egg laying begins ~3 h ASM.

After eggs have begun to move through the RT (12) and to be laid (3, 5, and 8 h ASM), the lumen of the uterus contracts back to resemble the uterine lumen of a virgin female (except when it contains an egg; Fig. 4 and Fig. S4). Interestingly, after the MP was expelled, uterine volume was smaller than the uterine volume of a virgin female (51% smaller at 5 h, 60.5% smaller at 3 h). We propose that uterine contraction could have any or all of the following purposes: (*i*) expelling the MP, (*ii*) tilting the uterus to make room for the ovulating egg and to affect the coiling of the oviduct (see below), and (*iii*) pushing the fertilized egg out of the uterus.

Analysis of 3D views from micro-CT scans of multiple samples also revealed postmating shifts in uterine position. By 5 h ASM, the anterior uterus has tilted dorsally and lies perpendicular to the anterior-posterior axis (Fig. 4). This tilt was also seen in one of the two females that lacked an egg in their uterus at 8 h ASM (Fig. 3*A*). Four other females scanned at 8 h ASM had an egg in their uterus (Fig. 4); these uteri were not tilted.

Seminal Proteins Modulate the Female's Uterine 3D Shape and Volume. Changes in uterine conformation are triggered by Acps (accessory gland proteins), the subclass of SFPs made by the male's accessory glands (22). To visualize effects of Acps on the uterus in situ, we mated females to males lacking Acps (50) (Table S1). In females mated to Acp-deficient males at 35 min ASM, the lumen of the anterior uterus remained tightly shut (Fig. 4, Acp^{-}). The posterior uterine lumen is filled with a compact ball of high density, representing the sperm mass and ejaculatory bulb proteins (Fig. 4, Acp^{-}). Previous studies using dissected tissues showed that one particular Acp, Acp36DE, necessary for sperm entry into storage and a component of the anterior MP (24, 25, 32), is also required to release a miduterine constriction (16). In contrast, another Acp, the "sex peptide," does not affect sperm entry into storage or uterine conformation (51). Our 3D views confirmed these results for both Acps (Fig. 4 and Fig. S3). For example, uteri of females whose mates lacked Acp36DE exhibited an hourglass shape at 35 min ASM, due to retention of a miduterine constriction (Fig. 4, Acp36DE^{-}). In these females, the bulk of the ejaculate remained

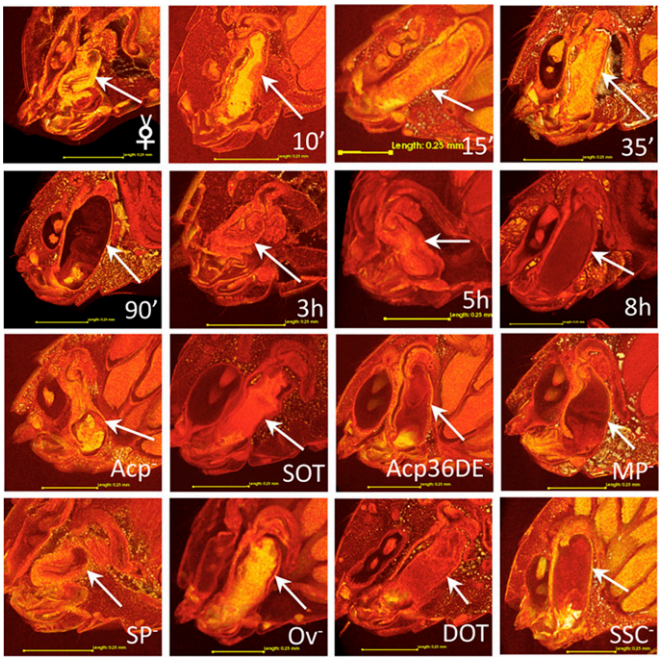

Fig. 4. Morphology of the uterus at the indicated times postmating. The uterus (arrows) progresses through stereotypic morphological changes triggered by SFP receipt. The 8-h time point shows an egg in the uterus. The lower eight panels show uterine morphology in the presence or absence of specific reproductive molecules or components (labels are as in Fig. 3; detailed definitions are provided in Table S1). (Scale bar: 0.25 mm.)

as a high-density mass in the posterior uterus. Given these confirmations, we then examined the role of another seminal protein, a product of the ejaculatory bulb that forms the posterior MP. Preventing MP formation (in mates of protein of the ejaculatory bulb (pEBme) knockdown males), the uterus took on a "swollen" appearance at 35 min ASM, with a distinct constriction in the anterior uterus (Fig. 4, MP^-). Thus, the MP also plays a role in the mating-induced uterine shape changes.

Although our data are snapshots into the postmated female RT, viewing them as a sequence of events over time leads to a model of uterine and oviduct positions and conformations that occur after a typical mating. In this light, our data suggest that the tilting and shape changes of the uterus can pull the oviduct, straightening the latter to allow egg movement, or can release tension, allowing the oviduct loop to reform, potentially impeding egg entry into the oviduct (see below). Consistent with this view, manipulations that alter uterine position and conformation often affected the oviduct's torsion or chirality. For example, in conjunction with the abnormal uterine conformation at 35 min ASM in the absence of all Acps or of Acp36DE, females showed no loop in the upper common oviduct (Fig. 3*B*, Acp^- and $Acp36DE^-$). Further, mates of pEBme knockdown males showed only partial looping of their oviduct (Fig. 3*B*, MP^-). In contrast, oviduct looping was normal in females mated to sperm-deficient males (SOT), as was uterine conformation, at 35 min ASM (Figs. 3*B* and 4, SOT). An exception to this correlation was that although removal of sex peptide from the ejaculate did not visibly affect uterine conformation, one mate of a sex peptide-null male had a nearly straight oviduct at 90 min ASM (Fig. 3*B*, SP^-), whereas the other showed the loop at this time.

Concurrent changes in the amount and release of neuromodulators in different regions of the female RT at different times postmating have been proposed to determine and coordinate RT functions (29). It is possible that these neuromodulatory changes cause the changes in conformation, volume, and position of the RT organs observed in our micro-CT scans.

Integrated Changes in the Female's Reproductive Tract Could Regulate Egg Transit. Normal female RTs rarely contain more than one transiting oocyte, and almost never more than two (12), suggesting that mechanisms coordinate the rate of egg release with the readiness of the uterus to accept an egg and allow its fertilization. We propose that the time course of conformational and positional changes that we observed could physically coordinate egg entry and movement through the RT, limiting the number of oocytes passing through the female RT.

The virgin fly's uterus is in the collapsed S-shape with a clockwise loop, and the upper common oviduct is looped counterclockwise (Fig. S6*A*). After mating, the uterus balloons to its largest size and, in conjunction, the oviduct loop relaxes (Fig. S6*B*; 90 min). After MP ejection, the uterus contracts, returning to the virgin conformation (Fig. S6*C*). The anterior end of the uterus tilts backward, pulling on the relaxed oviduct and elongating it (Fig. S6*D*). This elongation could make room for the next egg to ovulate into the lateral oviduct (Fig. S6*E*), coordinating egg release with the availability of a uterus ready to accept the egg. Next, the egg enters the relaxed uterus in position to be fertilized (Fig. S6*F*). The oviduct loop reforms (Fig. S6*G*), potentially blocking the next oocyte from prematurely entering the oviduct. When the egg is ready to be laid, the uterus contracts again to push the egg out (Fig. S6 *C* and *H*). This contraction tilts the uterus, again pulling on the oviduct and straightening it, facilitating entry of the next mature oocyte (Fig. S6 *D* and *E*). The cycle can then repeat, allowing continued coordination of oocyte release with uterine availability.

Initially, the movements occur in response to mating and are triggered by male-derived molecules, such as Acps and pEBme. However, the changes continue after 3 h ASM, by which time almost all SFPs have been expelled or degraded, suggesting that the female fly then assumes control of her RT conformations.

Interestingly, our scans of females mated to males lacking all Acps revealed that Acps, but not sperm, are involved in maintaining the appropriate timing of relaxation of the oviduct loop. In addition, SFPs with known roles in ovulation (ovulin) and those SFPs with roles in processes unrelated to ovulation (i.e., sperm storage; Acp36DE and pEBme) affected the conformation of the oviduct. The oviduct loop may be what causes the lumen of the upper common oviduct to be closed off in unmated flies (52). A constriction occurs between the common and lateral oviducts, the region in which we observed the oviduct loop in our scans. Future experiments are needed to determine whether there is a sphincter present in the oviduct or if the loop we have identified is sufficient to close the lumen of the oviduct.

Conclusions

In his 1493 anatomical sketch of the cross-section of a copulating man and woman entitled "The Copulation," Leonardo da Vinci studied human reproductive anatomy to understand better how human reproduction is coordinated. Following the same thought process, we performed high-resolution micro-CT scans of female *Drosophila* abdomens before, during, and after mating (Figs. 1–4 and Table S1) to visualize reproductive anatomy in situ to understand better how *Drosophila* reproduction is coordinated. We demonstrate that noninvasive 3D micro-CT scans provide a valuable tool with which to view the interrelationship between reproductive organs as female flies respond to mating and its chemical components. With this powerful 3D perspective, we observed (*i*) changes in the looping, opening/closing, and positioning of female RT organs during and after mating, and (*ii*) evidence for female RT wounding by the male aedeagus. Our data lead to a model for how successive tilting and relaxing/contracting of organs within the RT could lead to coordinated and optimal release and movement of oocytes through the tract, as well as expulsion of the MP. In addition, we defined roles for specific components of the ejaculate, and of female secretions and physiology, in modulating these movements. Future studies will uncover the detailed basis and regulation of these movements and contractions.

Materials and Methods

Flies. Canton-S (CS) males were used for the time course experiments, and CS females were used in all experiments except those involving the eggless (DOT) and SSC^- females (Table S1). Flies were collected as virgins and aged for 3–5 d before analysis. Details of generation of flies lacking specific male or female secretions or cells are provided in the *SI Materials and Methods*.

Sample Preparation, Fixation, and Iodine Staining. Samples were flash-frozen in liquid nitrogen at the indicated times. A slipknot made in a strand of human hair was tied around the neck of each fly and fed through a pipette tip, allowing the fly to be submerged in 4% (wt/vol) paraformaldehyde in 1× PBS overnight. Samples were then dehydrated through 20%, 50%, 75%, 90% (wt/vol), and 100% ethanol washes for 4–6 h each, and then stained in 3% (wt/vol) iodine (KI/I_2 at 2:1) in 100% ethanol for 24 h (53). Unless noted, all flies for a given time or treatment showed the same organ positioning and morphology. $n = 2$ for all times and treatments except the 8-h time point ($n = 6$).

Micro-CT Scans. Scans were performed at the Cornell University Biotechnology Resource Center Imaging Facility using a Zeiss Xradia 520 Versa X-ray instrument. For each dataset, 3,600 X-ray projections were digitized at 0.1° intervals over 360° using 80 kV and 7 W with a 2,000-ms exposure time. Reconstructions used a modified Feldkamp filtered back-projection algorithm yielding 1.8 μm *x*–*y*–*z* voxels (unless otherwise noted). The copulating pair was scanned at multiple scales using 400-nm, 700-nm, 1.4-μm, and 2.8-μm voxel sizes to capture small features and obtain larger contextual information.

Reconstruction and Visualization. The micro-CT data were analyzed with 2D and 3D techniques using the software program OsiriX (64-bit, version 5.8.5). All data presented, except for the uterine volume measurements and reconstructions, were analyzed using the "3D Volume Rendering" tool. This

method produces a digital reproduction of the sample with color and opacity based on tissue density that can be virtually rotated and dissected (i.e., sliced/cropped) from any arbitrary angle. Each sample was optimized for the contrast, color, and shading yielding the highest quality visualization of tissues. Tissue or the material surrounding the tract could be specifically enhanced or eliminated from view by adjusting the opacity of its density.

ACKNOWLEDGMENTS. We thank M. Shulman for the idea of using CT scans to visualize *Drosophila* postmating responses, J. Morin for help in learning the OsiriX analysis program, and A. McCune for computer access. We are grateful to N. Buchon, A. Dobson, and J. P. Masly for consultation on *Drosophila* gut and reproductive anatomy. We thank J. Morin, N. Buchon, M. Goldberg, members of the M.F.W. laboratory, and anonymous reviewers for helpful comments and advice, and L. Blondel for video-editing. This work was supported by NIH/National Institute of Child Health and Human Development Grant R01-HD038921 (to M.F.W.), National Science Foundation (NSF) Grant 0933921 (to M. Shulman and R. Harris-Warrick), NIH Grant S10OD012287 for instrumentation, and Weiss Fellowship funds (to M.F.W.). A.L.M. was a Biology Research Scholar supported by NSF Grant 0933921.

1. Avila FW, Sirot LK, LaFlamme BA, Rubinstein CD, Wolfner MF (2011) Insect seminal fluid proteins: Identification and function. *Annu Rev Entomol* 56:21–40.
2. Poiani A (2006) Complexity of seminal fluid: A review. *Behav Ecol Sociobiol* 60(3): 289–310.
3. Rodríguez-Martínez H, Kvist U, Ernerudh J, Sanz L, Calvete JJ (2011) Seminal plasma proteins: What role do they play? *Am J Reprod Immunol* 66(Suppl 1):11–22.
4. Druart X, et al. (2013) Proteomic characterization and cross species comparison of mammalian seminal plasma. *J Proteomics* 91:13–22.
5. Corrigan L, et al. (2014) BMP-regulated exosomes from Drosophila male reproductive glands reprogram female behavior. *J Cell Biol* 206(5):671–688.
6. Utleg AG, et al. (2003) Proteomic analysis of human prostasomes. *Prostate* 56(2): 150–161.
7. Katila T (2001) Sperm-uterine interactions: A review. *Anim Reprod Sci* 68(3-4): 267–272.
8. Wånggren K, Stavreus-Evers A, Olsson C, Andersson E, Gemzell-Danielsson K (2008) Regulation of muscular contractions in the human Fallopian tube through prostaglandins and progestagens. *Hum Reprod* 23(10):2359–2368.
9. Kunz G, et al. (1997) The uterine peristaltic pump. Normal and impeded sperm transport within the female genital tract. *Adv Exp Med Biol* 424:267–277.
10. Rubinstein CD, Wolfner MF (2013) Drosophila seminal protein ovulin mediates ovulation through female octopamine neuronal signaling. *Proc Natl Acad Sci USA* 110(43):17420–17425.
11. Ratto MH, et al. (2012) The nerve of ovulation-inducing factor in semen. *Proc Natl Acad Sci USA* 109(37):15042–15047.
12. Heifetz Y, Lung O, Frongillo EA, Wolfner MF (2000) The Drosophila seminal fluid protein Acp26Aa stimulates release of oocytes by the ovary. *Curr Biol* 10(2):99–102.
13. Heifetz Y, Vandenberg LN, Cohn HI, Wolfner MF (2005) Two cleavage products of the Drosophila accessory gland protein ovulin can independently induce ovulation. *Proc Natl Acad Sci USA* 102(3):743–748.
14. Pampalakis G, Sotiropoulou G (2007) Tissue kallikrein proteolytic cascade pathways in normal physiology and cancer. *Biochim Biophys Acta* 1776(1):22–31.
15. Rogers DW, et al. (2009) Transglutaminase-mediated semen coagulation controls sperm storage in the malaria mosquito. *PLoS Biol* 7(12):e1000272.
16. Avila FW, Wolfner MF (2009) Acp36DE is required for uterine conformational changes in mated Drosophila females. *Proc Natl Acad Sci USA* 106(37):15796–15800.
17. Dean MD (2013) Genetic disruption of the copulatory plug in mice leads to severely reduced fertility. *PLoS Genet* 9(1):e1003185.
18. Robertson SA (2007) Seminal fluid signaling in the female reproductive tract: Lessons from rodents and pigs. *J Anim Sci* 85(13, Suppl):E36–E44.
19. Findlay GD, Yi X, Maccoss MJ, Swanson WJ (2008) Proteomics reveals novel Drosophila seminal fluid proteins transferred at mating. *PLoS Biol* 6(7):e178.
20. Findlay GD, MacCoss MJ, Swanson WJ (2009) Proteomic discovery of previously unannotated, rapidly evolving seminal fluid genes in Drosophila. *Genome Res* 19(5): 886–896.
21. Yamamoto M-T, Takemori N (2010) Proteome profiling reveals tissue-specific protein expression in the male reproductive system of Drosophila melanogaster. *Fly (Austin)* 4(1):36–39.
22. Adams EM, Wolfner MF (2007) Seminal proteins but not sperm induce morphological changes in the Drosophila melanogaster female reproductive tract during sperm storage. *J Insect Physiol* 53(4):319–331.
23. Chapman T, et al. (2003) The sex peptide of Drosophila melanogaster: Female postmating responses analyzed by using RNA interference. *Proc Natl Acad Sci USA* 100(17):9923–9928.
24. Bloch Qazi MC, Wolfner MF (2003) An early role for the Drosophila melanogaster male seminal protein Acp36DE in female sperm storage. *J Exp Biol* 206(Pt 19): 3521–3528.
25. Neubaum DM, Wolfner MF (1999) Mated Drosophila melanogaster females require a seminal fluid protein, Acp36DE, to store sperm efficiently. *Genetics* 153(2):845–857.
26. Carvalho GB, Kapahi P, Anderson DJ, Benzer S (2006) Allocrine modulation of feeding behavior by the Sex Peptide of Drosophila. *Curr Biol* 16(7):692–696.
27. Apger-McGlaughon J, Wolfner MF (2013) Post-mating change in excretion by mated Drosophila melanogaster females is a long-term response that depends on sex peptide and sperm. *J Insect Physiol* 59(10):1024–1030.
28. Cognigni P, Bailey AP, Miguel-Aliaga I (2011) Enteric neurons and systemic signals couple nutritional and reproductive status with intestinal homeostasis. *Cell Metab* 13(1):92–104.
29. Heifetz Y, Lindner M, Garini Y, Wolfner MF (2014) Mating regulates neuromodulator ensembles at nerve termini innervating the Drosophila reproductive tract. *Curr Biol* 24(7):731–737.
30. Lung O, Wolfner MF (2001) Identification and characterization of the major Drosophila melanogaster mating plug protein. *Insect Biochem Mol Biol* 31(6-7):543–551.
31. Lung O, Wolfner MF (1999) Drosophila seminal fluid proteins enter the circulatory system of the mated female fly by crossing the posterior vaginal wall. *Insect Biochem Mol Biol* 29(12):1043–1052.
32. Bertram MJ, Neubaum DM, Wolfner MF (1996) Localization of the Drosophila male accessory gland protein Acp36DE in the mated female suggests a role in sperm storage. *Insect Biochem Mol Biol* 26(8-9):971–980.
33. Gilchrist AS, Partridge L (2000) Why it is difficult to model sperm displacement in Drosophila melanogaster: The relation between sperm transfer and copulation duration. *Evolution* 54(2):534–542.
34. Manier MK, et al. (2010) Resolving mechanisms of competitive fertilization success in Drosophila melanogaster. *Science* 328(5976):354–357.
35. Kamimura Y (2010) Copulation anatomy of Drosophila melanogaster (Diptera: Drosophilidae): Wound-making organs and their possible roles. *Zoomorphology* 129(3): 163–174.
36. Pilpel N, Nezer I, Applebaum SW, Heifetz Y (2008) Mating-increases trypsin in female Drosophila hemolymph. *Insect Biochem Mol Biol* 38(3):320–330.
37. Bono JM, Matzkin LM, Kelleher ES, Markow TA (2011) Postmating transcriptional changes in reproductive tracts of con- and heterospecifically mated Drosophila mojavensis females. *Proc Natl Acad Sci USA* 108(19):7878–7883.
38. Lung O, Kuo L, Wolfner MF (2001) Drosophila males transfer antibacterial proteins from their accessory gland and ejaculatory duct to their mates. *J Insect Physiol* 47(6): 617–622.
39. Fedorka KM, Linder JE, Winterhalter W, Promislow D (2007) Post-mating disparity between potential and realized immune response in Drosophila melanogaster. *Proc Biol Sci* 274(1614):1211–1217.
40. Kapelnikov A, et al. (2008) Mating induces an immune response and developmental switch in the Drosophila oviduct. *Proc Natl Acad Sci USA* 105(37):13912–13917.
41. Gendrin M, Welchman DP, Poidevin M, Hervé M, Lemaitre B (2009) Long-range activation of systemic immunity through peptidoglycan diffusion in Drosophila. *PLoS Pathog* 5(12):e1000694.
42. Chapman T, Neubaum DM, Wolfner MF, Partridge L (2000) The role of male accessory gland protein Acp36DE in sperm competition in Drosophila melanogaster. *Proc Biol Sci* 267(1448):1097–1105.
43. Heifetz Y, Tram U, Wolfner MF (2001) Male contributions to egg production: the role of accessory gland products and sperm in Drosophila melanogaster. *Proc Biol Sci* 268(1463):175–180.
44. Kambysellis MP (1968) Comparative Studies of Oogenesis and Egg Morphology Among Species of the Genus Drosophila (University of Texas, Austin, TX), Publ No 6818.
45. Clements A (1992) *Development, Nutrition and Reproduction* (Cabi Publishing, Wallingford, UK).
46. Sun J, Spradling AC (2013) Ovulation in Drosophila is controlled by secretory cells of the female reproductive tract. *eLife* 2:e00415.
47. Schnakenberg SL, Matias WR, Siegal ML (2011) Sperm-storage defects and live birth in Drosophila females lacking spermathecal secretory cells. *PLoS Biol* 9(11):e1001192.
48. Herndon LA, Wolfner MF (1995) A Drosophila seminal fluid protein, Acp26Aa, stimulates egg laying in females for 1 day after mating. *Proc Natl Acad Sci USA* 92(22): 10114–10118.
49. Boswell RE, Mahowald AP (1985) tudor, a gene required for assembly of the germ plasm in Drosophila melanogaster. *Cell* 43(1):97–104.
50. Chow CY, Avila FW, Clark AG, Wolfner MF (2015) Induction of excessive endoplasmic reticulum stress in the Drosophila male accessory gland results in infertility. *PLoS ONE* 10(3):e0119386.
51. Avila FW, Ravi Ram K, Bloch Qazi MC, Wolfner MF (2010) Sex peptide is required for the efficient release of stored sperm in mated Drosophila females. *Genetics* 186(2): 595–600.
52. Kapelnikov A, Rivlin PK, Hoy RR, Heifetz Y (2008) Tissue remodeling: A mating-induced differentiation program for the Drosophila oviduct. *BMC Dev Biol* 8:114.
53. Metscher BD (2009) MicroCT for comparative morphology: Simple staining methods allow high-contrast 3D imaging of diverse non-mineralized animal tissues. *BMC Physiol* 9:11.
54. Ryoo HD, Domingos PM, Kang MJ, Steller H (2007) Unfolded protein response in a Drosophila model for retinal degeneration. *EMBO J* 26(1):242–252.
55. Xue L, Noll M (2002) Dual role of the Pax gene paired in accessory gland development of Drosophila. *Development* 129(2):339–346.
56. Liu H, Kubli E (2003) Sex-peptide is the molecular basis of the sperm effect in Drosophila melanogaster. *Proc Natl Acad Sci USA* 100(17):9929–9933.